

# Evolution behavior of oxide inclusions in Si-Mn deoxidized steel during billet heating process

X.-L. Nie <sup>a</sup>, Q. Xu <sup>a</sup>, X. Xie <sup>a</sup>, J.-L. Li <sup>\*,a,b</sup>

<sup>a</sup> Key Laboratory for Ferrous Metallurgy and Resources Utilization of Ministry of Education, Wuhan University of Science and Technology, Wuhan, 430081, Hubei, China

<sup>b</sup> Hubei Provincial Key Laboratory for New Processes of Ironmaking and Steelmaking, Wuhan University of Science and Technology, Wuhan, 430081, Hubei, China  
Xinlong Nie, E-mail address: 1946846620@qq.com

Qi Xu, E-mail address: xuqi@wust.edu.cn

Xiao Xie, E-mail address: xiexiao@wust.edu.cn

\* Jianli Li, E-mail address: [jli@wust.edu.cn](mailto:jli@wust.edu.cn)

(Received 09 January 2025; Accepted 14 June 2025)

## Abstract

To minimize the impact of oxide inclusions on the quality of Si-Mn deoxidized steel, the effects of heat treatment temperature and holding time on inclusion composition and morphology were studied. LX82A billets were heated isothermally at 1000, 1100, and 1200°C for 8, 10, and 12 hours, respectively. The experimental results show that as the heat treatment temperature increases, calcium treatment and the reduction of the  $w(\text{Al}_2\text{O}_3 + \text{MgO}) / w(\text{SiO}_2 + \text{MnO})$  ratio enhance the deformability of oxide inclusions. This causes a gradual transition in inclusion shape from oval to round. At 1200°C, the oxide inclusions are predominantly regular and round. Increasing heat treatment temperature and holding time shifts the oxide inclusions in Si-Mn deoxidized steel from the CaO-SiO<sub>2</sub>-Al<sub>2</sub>O<sub>3</sub> system to the MnO-SiO<sub>2</sub>-Al<sub>2</sub>O<sub>3</sub> system. At a constant temperature, the highest inclusion transformation rate and most uniform composition occur with a 10-hour holding time. At 1200°C, an alternative calcium treatment and the steel matrix-inclusion interface reaction increase the MnO content at the interface, reducing the manganese content in the steel and forming a Mn-depleted zone. This decreases austenite stability, enhances ferrite nucleation, and improves steel quality and performance. Therefore, controlling the heat treatment temperature around 1200°C is crucial.

**Keywords:** Si-Mn deoxidized steel; Oxide inclusion; Heat treatment; Temperature; Holding time; Composition changes

## 1 Introduction

Non-metallic inclusions can adversely affect the plasticity, toughness, fatigue resistance and ductility of steel, which will eventually lead to the reduction of steel quality and service life. The inclusions mainly include oxides, sulfides, nitrides, etc., which are usually formed during the steelmaking process due to the addition of deoxidizers, the involvement of slag and the change of element solubility<sup>[1-8]</sup>. Si-Mn

deoxidation process can avoid the formation of high melting point and hard inclusions ( $\text{Al}_2\text{O}_3$  etc.), so it is widely used in the production of spring steel and tire cord steel<sup>[9-12]</sup>.

Due to the interface reaction between steel matrix and inclusions, the composition and morphology of inclusions in Si-Mn deoxidized steel will change after the heat treatment. In addition, near the interface between steel matrix and oxide inclusions, silicon-manganese oxide particles gradually precipitate, resulting in the decrease of manganese content in the alloy in this area, thus forming a Mn-depleted zone. The presence of a Mn-depleted zone reduces the stability of austenite and increases the driving force for ferrite nucleation, which facilitates the occurrence of intergranular ferrite (IGF) nucleation, thereby improving the steel's performance by refining the grain structure and enhancing its strength and toughness. The increase in MnO content in non-metallic inclusions also indicates an expansion of the Mn-depleted zone width<sup>[1, 13]</sup>. Studies have shown that it was feasible to influence and control inclusions in steel through heat treatment processes. Heat treatment process can lead to the modification of original inclusions, the precipitation of new inclusions, and changes in the microstructure and composition of the steel matrix<sup>[14-17]</sup>. Therefore, it is important to investigate the effects of heat treatment processes on the evolution of inclusions.

Liu et al.<sup>[1]</sup> investigated the changes in the chemical composition of Fe-Mn-Si alloys and  $\text{CaO-SiO}_2\text{-Al}_2\text{O}_3\text{-MgO-MnO}$  oxides during heat treatment at 1000 °C and 1200 °C. The study revealed that, compared to the "solid-solid" reaction between the alloy and oxide at 1000 °C, the "solid-liquid" reaction at 1200 °C resulted in a further increase in the Mn content near the alloy interface and a further decrease in the Si content. The total contents of MnO and  $\text{SiO}_2$  in the oxide decreased and increased, respectively. Furthermore, it was determined that the MnO content in the oxide and the Si content in the alloy are the driving forces behind the interfacial reactions. Kim et al.<sup>[13]</sup> investigated the reaction between  $\text{MnO-SiO}_2\text{-FeO}$  oxides and Fe-Mn-Si alloys after a 10-hour holding at 1200 °C using a diffusion couple method. The study showed that when the oxides interact with silicon-manganese deoxidized steel under heating conditions, the FeO content in the oxides increased near the interface, which caused fluctuations in the Mn and Si content in the alloy near the interface. Shibata et al.<sup>[18]</sup> used the diffusion couple method to observe the solid-state reactions between Fe-Cr alloys and  $\text{MnO-SiO}_2$  oxides after heat treatment at 1200 °C. The study revealed that when the Si content in the alloy was low,  $\text{MnO-SiO}_2$  inclusions could transform into  $\text{MnO-Cr}_2\text{O}_3$  inclusions. These fine  $\text{MnO-Cr}_2\text{O}_3$  inclusions exhibited a strong pinning effect, which suppressed grain boundary migration, effectively preventing grain coarsening. As a result, the grains remained extremely fine, contributing to enhanced strength and toughness of the material. Choi et al.<sup>[19]</sup> investigated the evolution behavior of inclusions in Al-Ti deoxidized alloys under heat treatment at 1200 °C. They found that the initial inclusions formed in alloys with different Al and Ti contents, such as  $\text{Al}_2\text{O}_3$ , Al-Ti-O, and TiOx, transformed into Al-Ti-Fe-O, Al-Fe-O, and Fe-Ti-O inclusions, respectively. This transformation contributed to improved processing performance, ductility, and corrosion resistance of the steel.

The studies mentioned above have demonstrated that heat treatment temperature can alter the composition of inclusions, thereby enhancing the performance and quality of steel. Shibata et al.<sup>[18]</sup> further observed that the average composition of oxide inclusions also changes with variations in heat treatment time. Therefore, the combined effects of temperature and time during heat treatment are crucial in determining the composition and morphology of inclusions, which in turn influences the overall performance of the steel. However, previous research has not thoroughly explored the

compositional variations of non-metallic inclusions under different heat treatment temperatures and holding times. The main products of silicomanganese deoxidation are MnO and SiO<sub>2</sub>. Most of the literature on non-metallic inclusions in silicomanganese deoxidized steels focuses on ternary systems and indirectly reflects compositional changes of non-metallic inclusions through the diffusion couple method. In practical silicomanganese deoxidized steels, however, non-metallic inclusions are relatively small in size and often exist in the form of a quinary system (CaO-SiO<sub>2</sub>-Al<sub>2</sub>O<sub>3</sub>-MgO-MnO). Therefore, it is essential to study the effects of different heating temperatures and holding times on the composition of CaO-SiO<sub>2</sub>-Al<sub>2</sub>O<sub>3</sub>-MgO-MnO inclusions in silicomanganese deoxidized steels. In the current work, the Si-Mn deoxidized steel LX82A billets are isothermal heating at 1000 ~1200 °C for 8~12h respectively to investigate the effects of heat treatment temperature and isothermal heating time on the composition and morphology of inclusions. The morphology and composition of inclusions in the LX82A billets are detected by SEM-EDS. The aim of this study is to explore optimal heat treatment conditions and provide theoretical insights for better controlling the composition and morphology of non-metallic inclusions in silicon-manganese deoxidized steel. By appropriately managing heat treatment conditions, the quality of the steel can be improved. The research findings contribute to optimizing the inclusion plasticization control process in Si-Mn deoxidized steel, thereby minimizing the impact of inclusions on the quality and performance of steel products.

## 2 Experimental methods

### 2.1 Materials

In this experiment, LX82A Si-Mn deoxidized billets were used to sample molten steel from the tundish. The chemical composition was analyzed through spectroscopy, as presented in Table 1. The oxygen content in the steel is 11 ppm. The main production process for LX82A wire cord steel begins with raw material preparation, where scrap steel, iron ore, and alloy materials are melted into molten steel in a converter. Subsequently, the molten steel undergoes refining before entering the continuous casting process, where it is cast into slabs of a specific thickness and width through continuous casting. After initial cooling, the cast billets undergo surface treatment or finishing through the hot rolling process to improve their surface quality and dimensional accuracy, ultimately becoming suitable raw materials for subsequent cold drawing or heat treatment processes. Table 1 shows the chemical composition of the tested steel.

Table 1 The chemical composition of the tested steel(wt%)

C	Si	Mn	P	S	Cr	Ni	Mo	Cu	Al
0.813	0.180	0.511	0.014	0.011	0.035	0.011	0.0017	0.024	0.0012

### 2.2 Heat treatment experiment

The Si-Mn deoxidized steel LX82A slab was cut into steel samples with dimensions of 10 mm × 10 mm × 10 mm. These samples were then heated in a high-temperature furnace at a rate of 7°C/min to temperatures of 1000°C, 1100°C, and 1200°C, with holding times of 8 hours, 10 hours, and 12 hours, respectively. After the heat treatment, to minimize any internal reactions that might occur during the cooling process, the steel samples were quickly removed from the furnace and quenched in water to room temperature. The steel sample and the steel sample after heat treatment were inlaid, and the surface was polished on the sandpaper of 400,800,1200,1500 and 2000 mesh in turn, and finally polished to the mirror surface under the metallographic polishing machine. After cleaning, blow dry and dry, put it in a vacuum dish for use.

The number, morphology, and composition of inclusions in steel samples were analyzed using scanning electron microscopy (SEM) combined with energy dispersive spectroscopy (EDS). Each inclusion detected by the SEM was manually reviewed and analyzed to eliminate errors, such as holes or dust. The inclusions on a single polished surface of each sample were detected, and non-oxide inclusions, as well as oxide inclusions smaller than 1  $\mu\text{m}$ , were excluded to ensure the accuracy of the measurement results. Each sample was statistically analyzed for 30~40 oxide inclusions that met the specified conditions. The elemental contents of the oxide inclusions, as measured by SEM-EDS, were then converted into compound components using the following methods: (1) Mn preferentially combined with S, and the MnS content was calculated based on the measured S content; (2) The remaining Mn, along with other elements such as Ca, Si, Al, and Mg in the oxide, were directly converted into MnO, CaO, SiO<sub>2</sub>, Al<sub>2</sub>O<sub>3</sub>, and MgO according to their respective contents.

### 3 Results

#### 3.1 The initial oxide inclusions in the billet

There are mainly two types of inclusions in the Si-Mn deoxidized steel LX82A billet before heat treatment. The main inclusions in the billet are composite oxide inclusions of the CaO-SiO<sub>2</sub>-Al<sub>2</sub>O<sub>3</sub>-MgO-MnO system. The others are MnS inclusions with various shapes. Prior to heat treatment, the CaO-SiO<sub>2</sub>-Al<sub>2</sub>O<sub>3</sub>-MgO-MnO oxide inclusions in the LX82A silicon-manganese deoxidized steel predominantly exhibit an elliptical and regular shape, with sizes generally ranging from 2 to 3  $\mu\text{m}$ , as shown in Figure 1. In addition, a small quantity of oxide inclusions approximately 10  $\mu\text{m}$  in size was observed in the steel sample prior to heat treatment. These inclusions have a shape similar to those of the 2–3  $\mu\text{m}$  inclusions, being elliptical and regular, with a distinct dark SiO<sub>2</sub> component present, as shown in Figure 2.

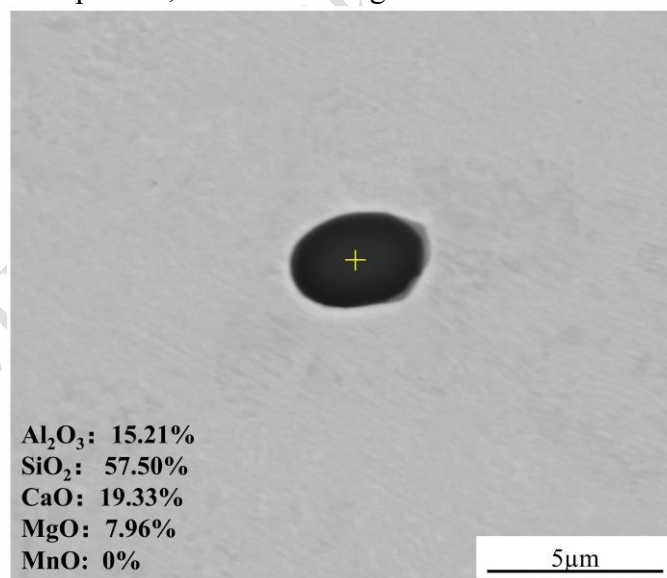


Fig.1 Morphology characteristics of 2-3 $\mu\text{m}$  oxide inclusions in LX82A Si-Mn deoxidized steel before heat treatment

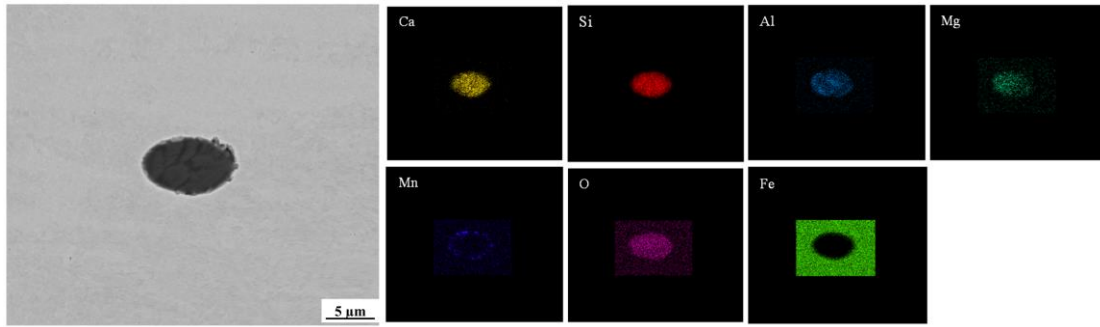


Fig.2 Morphology and composition surface scanning characteristics of oxide inclusions about 10  $\mu\text{m}$  in LX82A Si-Mn deoxidized steel before heat treatment

According to relevant literature<sup>[20, 21]</sup>, the oxide inclusions in Si-Mn deoxidized steel can be classified into two categories: the CaO-SiO<sub>2</sub>-Al<sub>2</sub>O<sub>3</sub> system and the MnO-SiO<sub>2</sub>-Al<sub>2</sub>O<sub>3</sub> system. When the mole fraction of CaO is greater than MnO, the inclusions are divided into CaO-SiO<sub>2</sub>-Al<sub>2</sub>O<sub>3</sub> inclusions. On the contrary, when the mole fraction of MnO is greater than CaO, the inclusions are divided into MnO-SiO<sub>2</sub>-Al<sub>2</sub>O<sub>3</sub> inclusions. Based on this, we used the thermodynamic software FactSage 8.0 Phase Diagram module to calculate and plot the ternary phase diagrams of CaO-SiO<sub>2</sub>-Al<sub>2</sub>O<sub>3</sub> and MnO-SiO<sub>2</sub>-Al<sub>2</sub>O<sub>3</sub>. The composition of the inclusions, as determined by statistical analysis, was then plotted on the respective phase diagrams of CaO-SiO<sub>2</sub>-Al<sub>2</sub>O<sub>3</sub> and MnO-SiO<sub>2</sub>-Al<sub>2</sub>O<sub>3</sub>. The effects of heating temperature and holding time on the oxide inclusion were observed. The composition distribution of the oxide inclusions before heat treatment is shown in Figure 3.

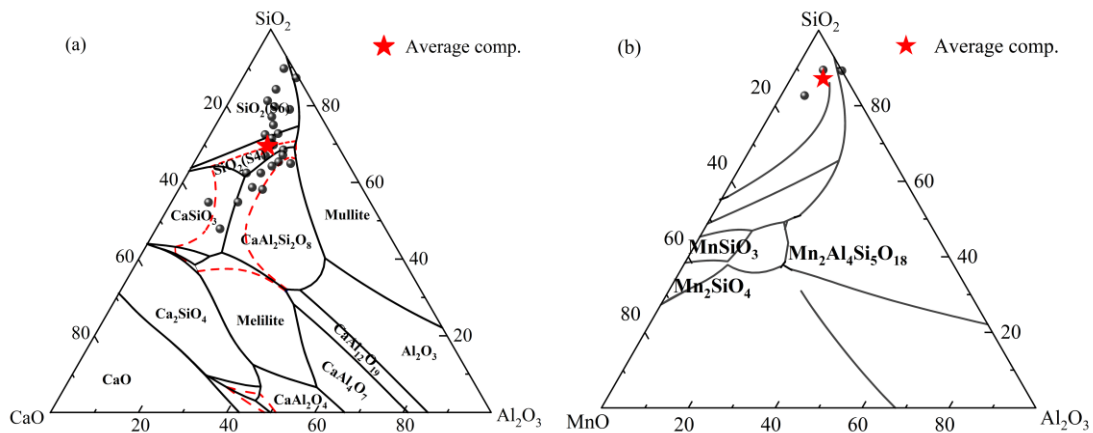


Fig. 3 Composition distribution of oxide inclusions in (a) CaO-SiO<sub>2</sub>-Al<sub>2</sub>O<sub>3</sub> and (b) MnO-SiO<sub>2</sub>-Al<sub>2</sub>O<sub>3</sub> ternary phase diagrams before heat treatment.

As shown in Figures 3(a) and 3(b), the majority of the oxide inclusions, accounting for 87.5%, fall within the CaO-SiO<sub>2</sub>-Al<sub>2</sub>O<sub>3</sub> ternary phase diagram without heat treatment or heat preservation. In contrast, only a small fraction of the oxide inclusions, 12.5%, fall within the MnO-SiO<sub>2</sub>-Al<sub>2</sub>O<sub>3</sub> ternary phase diagram. This indicates that the oxide inclusions in Si-Mn deoxidized steel LX82A billet are mainly CaO-SiO<sub>2</sub>-Al<sub>2</sub>O<sub>3</sub> system inclusions before the heat treatment process. The SiO<sub>2</sub> content in the composite oxide inclusions is high.

### 3.2 Morphology characteristics of oxide inclusions after heat treatment

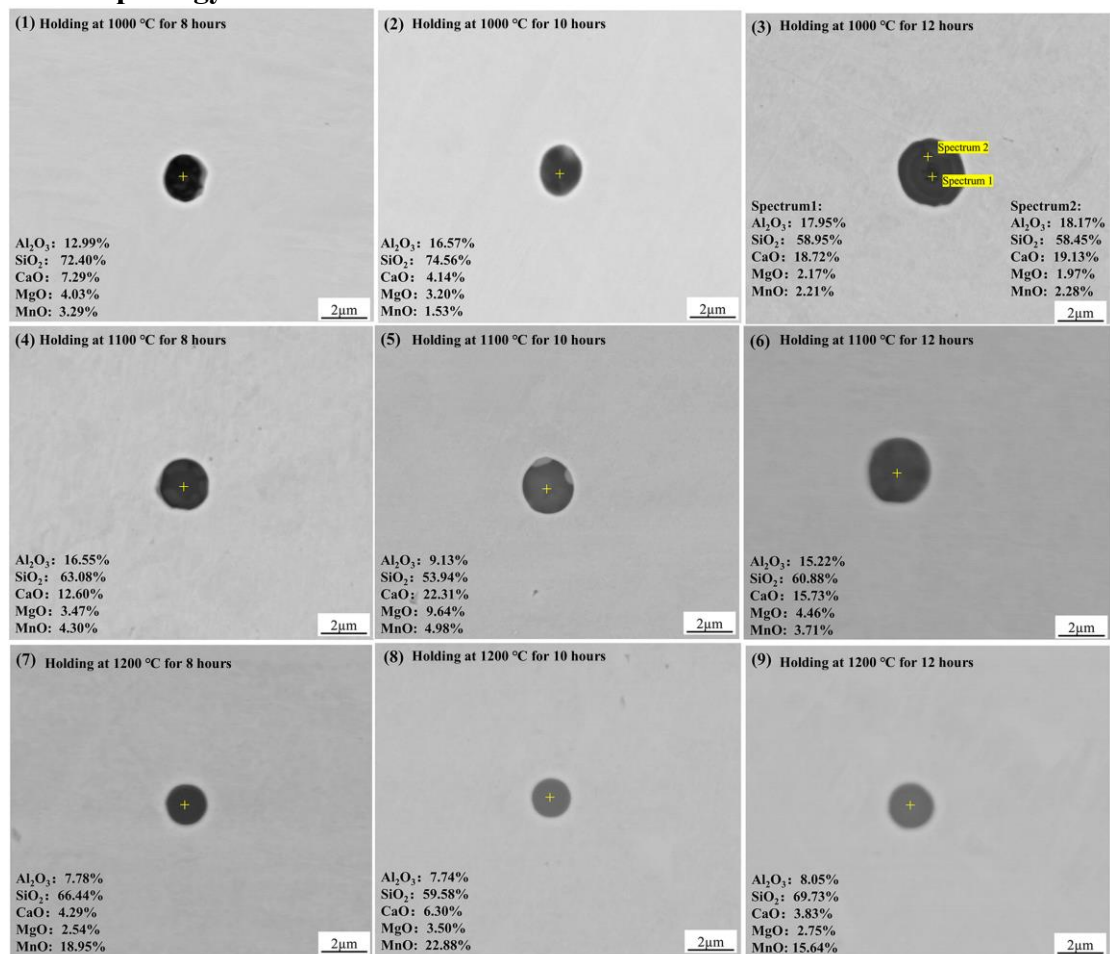


Fig.4 Morphology of oxide inclusions in LX82A steel under different heat treatment conditions

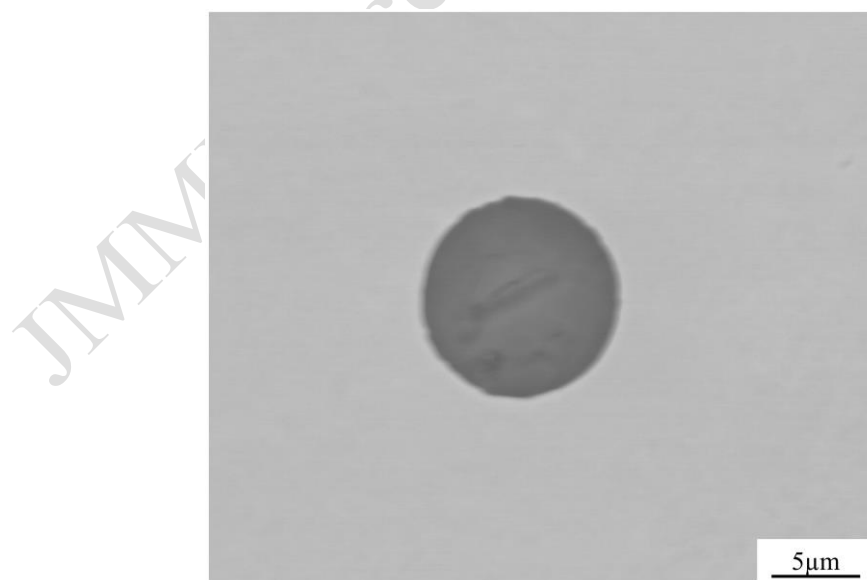


Fig. 5 The morphology of about 10 μm oxide inclusions in LX82A Si-Mn deoxidized steel after heat treatment at 1200 °C

As shown in Figure 4, with an increase in heat treatment temperature, the shape of



oxide inclusions in the steel gradually transitions from elliptical to more spherical. At a heating temperature of 1200°C, the oxide inclusions in the steel predominantly take the form of regular spheres. The holding time, however, has little effect on the morphological change of the oxide inclusions. Furthermore, as the temperature rises, the proportion of MnO in the oxide inclusions gradually increases, with the most significant change occurring at 1200°C, where the mass fraction of MnO reaches approximately 20%. A comparison of the oxide inclusion morphology in Figures 2 and 5 reveals that oxide inclusions of approximately 10 µm in size undergo a similar transformation from elliptical to regular spherical shapes after heat treatment at 1200°C, which is consistent with the observations in Figure 4.

### 3.3 Composition evolution of oxide inclusions after heat treatment

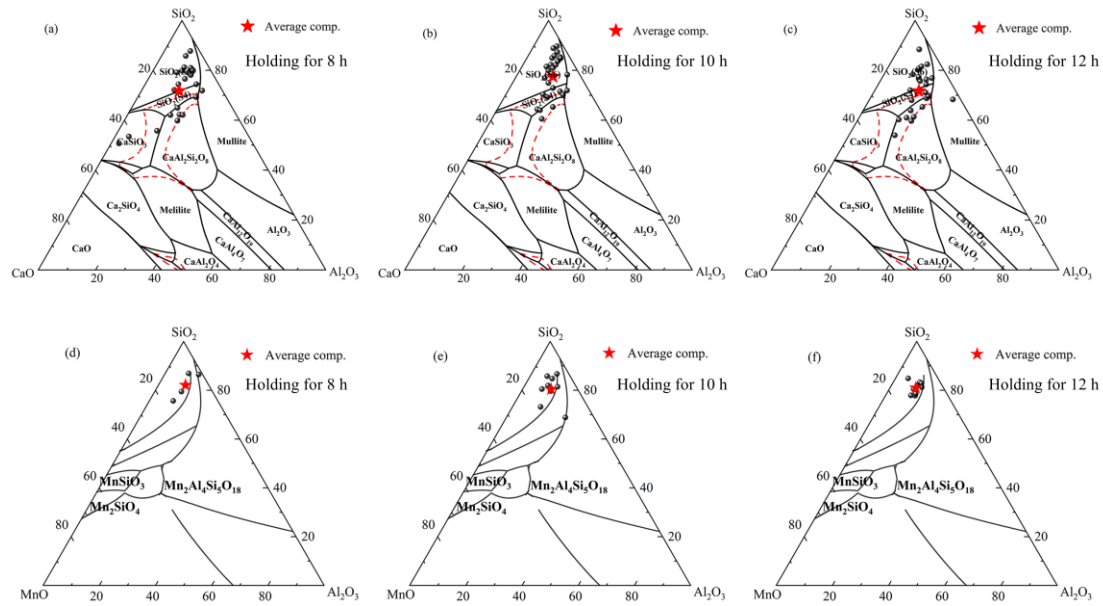


Fig.6 The composition distribution of oxide inclusions in  $\text{CaO-SiO}_2\text{-Al}_2\text{O}_3$  and  $\text{MnO-SiO}_2\text{-Al}_2\text{O}_3$  ternary phase diagrams after heat treatment at 1000 °C

A comparison of the inclusion compositions in the  $\text{CaO-SiO}_2\text{-Al}_2\text{O}_3$  ternary phase diagram for Figures 6(a), (b), and (c) reveals that, under heat treatment at 1000°C, the distribution of oxide inclusions in the ternary phase diagram shifts upward to varying extents after holding for 8, 10, and 12 hours. This indicates a gradual increase in the  $\text{SiO}_2$  content, with the most pronounced change observed after holding for 10 hours at 1000°C. Comparing the oxide inclusions in the  $\text{MnO-SiO}_2\text{-Al}_2\text{O}_3$  ternary phase diagram, it is observed that at a heat treatment temperature of 1000°C, as the holding time is extended from 8 hours to 10 hours and 12 hours, the number of inclusions within the  $\text{MnO-SiO}_2\text{-Al}_2\text{O}_3$  ternary phase diagram increases. Consequently, the percentage of these inclusions relative to the total increases from 16.67% to 28.21% and 27.78%, respectively. This indicates that with the increase in holding time after heat treatment at 1000°C, a portion of the inclusion components transform, leading to a higher molar fraction of MnO compared to CaO, i.e., an increase in the mass fraction of MnO. Furthermore, a comparison of the oxide inclusions in the  $\text{MnO-SiO}_2\text{-Al}_2\text{O}_3$  ternary phase diagram (Figures 6(d), (e), (f)) reveals that as the holding time increases, the inclusions become more concentrated in the phase diagram. This suggests that under 1000°C heat treatment, the composition of oxide inclusions becomes more

homogeneous with prolonged holding time.

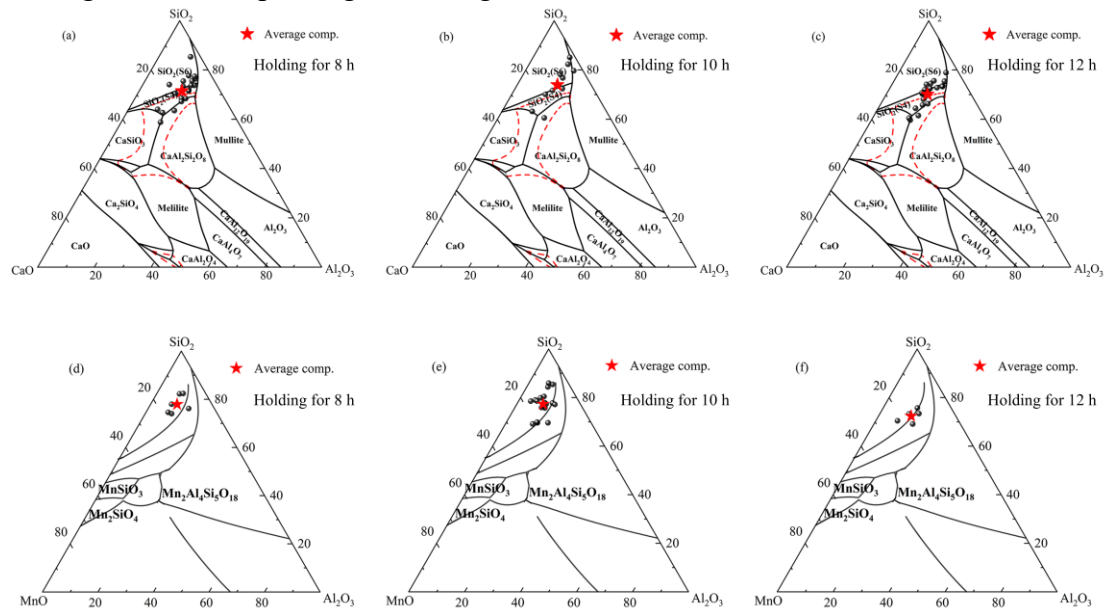


Fig.7 The composition distribution of oxide inclusions in  $\text{CaO-SiO}_2\text{-Al}_2\text{O}_3$  and  $\text{MnO-SiO}_2\text{-Al}_2\text{O}_3$  ternary phase diagrams after heat treatment at  $1100^\circ\text{C}$

When the steel sample is heated to  $1100^\circ\text{C}$ , it is observed that at holding times of 8 hours and 12 hours, oxide inclusions from the  $\text{CaO-SiO}_2\text{-Al}_2\text{O}_3$  system are dominant. However, at a holding time of 10 hours, inclusions from the  $\text{MnO-SiO}_2\text{-Al}_2\text{O}_3$  system become the predominant type. Comparing Figures 7(d), (e), and (f), it can be observed that at a heat treatment temperature of  $1100^\circ\text{C}$ , the transition from the  $\text{CaO-SiO}_2\text{-Al}_2\text{O}_3$  system to the  $\text{MnO-SiO}_2\text{-Al}_2\text{O}_3$  system shows the most significant change when the holding time is extended from 8 hours to 10 hours. During this period, the percentage of inclusions increased from 25% to 60.61%. However, when the holding time is extended to 12 hours, the percentage of  $\text{MnO-SiO}_2\text{-Al}_2\text{O}_3$  inclusions relative to the total number decreases to 22.58%, with minimal change compared to the 8-hour holding time. Comparing Figs. 6(b) and (e) with Figs. 7(b) and (e), it can be observed that when the holding time is kept constant at 10 hours and the heat treatment temperature is increased from  $1000^\circ\text{C}$  to  $1100^\circ\text{C}$ , a significant portion of the inclusions transition from the  $\text{CaO-SiO}_2\text{-Al}_2\text{O}_3$  system to the  $\text{MnO-SiO}_2\text{-Al}_2\text{O}_3$  system. As a result, the proportion of  $\text{MnO-SiO}_2\text{-Al}_2\text{O}_3$  inclusions increases from 28.21% to 60.61%. This suggests that temperature plays an important role in the transformation of oxide inclusions in silicon-manganese deoxidized steel.



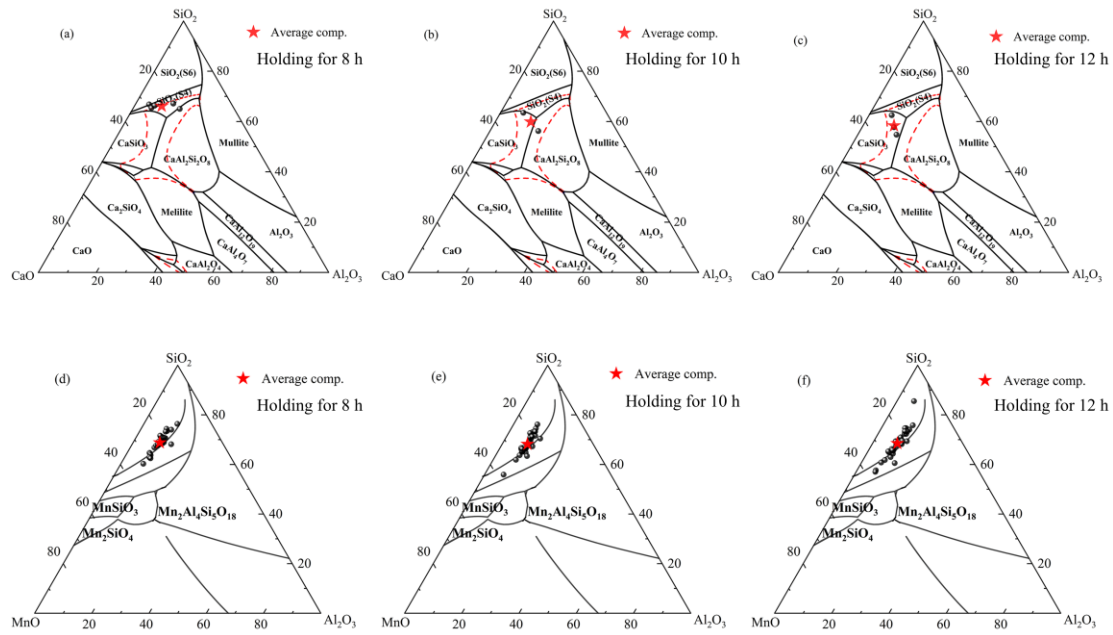


Fig.8 The composition distribution of oxide inclusions in  $\text{CaO-SiO}_2\text{-Al}_2\text{O}_3$  and  $\text{MnO-SiO}_2\text{-Al}_2\text{O}_3$  ternary phase diagrams after heat treatment at  $1200^\circ\text{C}$

Comparing Fig. 3 with Fig. 8, it is evident that when the steel sample is heated to  $1200^\circ\text{C}$ , regardless of whether the holding time is 8 hours, 10 hours, or 12 hours, most of the oxide inclusions have transitioned from the  $\text{CaO-SiO}_2\text{-Al}_2\text{O}_3$  system to the  $\text{MnO-SiO}_2\text{-Al}_2\text{O}_3$  system, compared to the sample before heat treatment. The proportion of  $\text{MnO-SiO}_2\text{-Al}_2\text{O}_3$  inclusions in the total has exceeded 80%. The highest transformation occurs with a holding time of 10 hours, where  $\text{MnO-SiO}_2\text{-Al}_2\text{O}_3$  inclusions account for 91.89% of the total. In comparison to the  $\text{MnO-SiO}_2\text{-Al}_2\text{O}_3$  inclusions formed at  $1000^\circ\text{C}$  and  $1100^\circ\text{C}$ , the oxide inclusions after heat treatment at  $1200^\circ\text{C}$  are more concentrated within the ternary phase diagram of the  $\text{MnO-SiO}_2\text{-Al}_2\text{O}_3$  system. This indicates that the composition of oxide inclusions after heat treatment at  $1200^\circ\text{C}$  is more uniform. Figs. 6-8 demonstrate that, when the heat treatment temperature is held constant, the inclusion transformation rate is highest and the inclusion composition is more uniform when the holding time is 10 hours.

By comparing the aforementioned ternary phase diagrams, it can be observed that under different heat treatment conditions, the MnO and  $\text{SiO}_2$  contents in the inclusions exhibit significant changes. However, the inclusions still contain certain amounts of MgO. The ternary systems in Figures 6 to 8 are normalized based on the exclusion of MgO. Previous studies have rarely investigated the variation of the five components of oxide inclusions in Si-Mn deoxidized steel under different heat treatment conditions<sup>[22, 23]</sup>. Therefore, to further explore the effects of different heat treatment temperatures and holding times on the composition of the five-component oxide inclusions, the following discussion will focus on how these components change in the LX82A Si-Mn deoxidized steel under the three selected heating temperatures and holding times in this experiment, and the influence of heating temperature and holding time will be explored.

## 4 Discussion

### 4.1 Changes of the composition of CaO-SiO<sub>2</sub>-Al<sub>2</sub>O<sub>3</sub>-MgO-MnO composite oxide inclusions under different heat treatment conditions

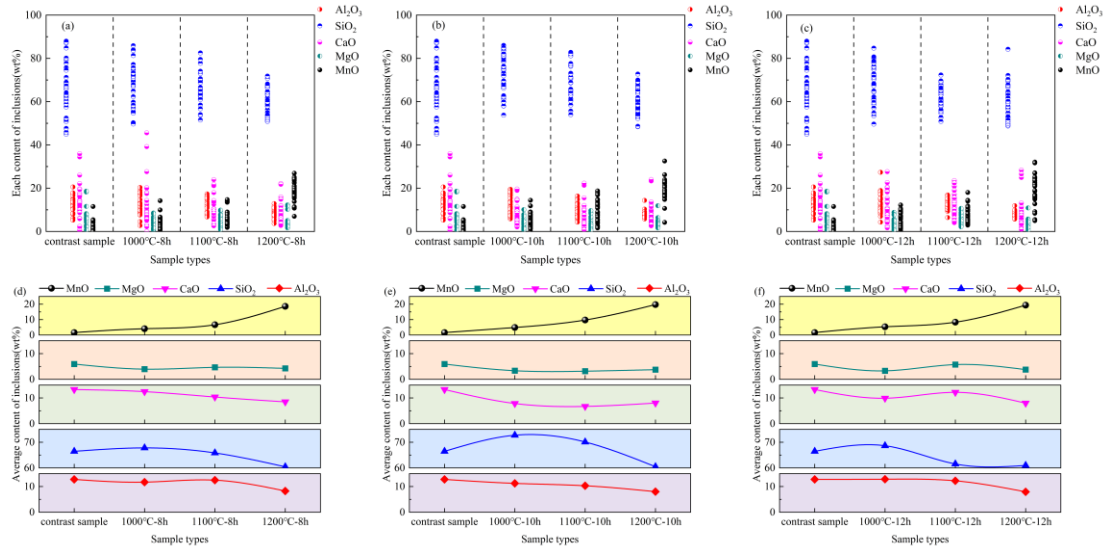


Fig. 9 Variation of the five components and their average compositions of oxide inclusions in LX82A steel with heating temperature, at holding times of (a, d) 8 hours, (b, e) 10 hours, and (c, f) 12 hours.

As shown in Figures 9(a) and (d), the MnO content in the oxide inclusions prior to heat treatment is generally below 5 wt%, with an average content of approximately 1.6 wt%. Under the condition of an 8-hour holding time, as the heating temperature increases, the mass fraction of MnO in the oxide inclusions continuously rises. When the temperature reaches 1200°C, the average content increases to 18.6 wt%. In contrast, the CaO content decreases with increasing heating temperature, with the average content dropping from an initial value of 13.2 wt% to 12.4 wt%, 10.3 wt%, and 8.5 wt%, respectively. The SiO<sub>2</sub> content exhibits a trend of first increasing and then decreasing with the rise in heating temperature. When the control sample undergoes isothermal heating at 1000°C for 8 hours, the average SiO<sub>2</sub> content in the steel increases from 66.4 wt% to 67.8 wt%, while the average MgO content decreases from 5.9 wt% to 3.9 wt%. As the heating temperature increases to 1100°C and 1200°C, the average SiO<sub>2</sub> content decreases to 65.8 wt% and 60.4 wt%, respectively, with no significant change observed in the average MgO content. After isothermal heating at 1000°C and 1100°C for 8 hours, the Al<sub>2</sub>O<sub>3</sub> content shows no significant change. However, when the heating temperature increases to 1200°C, the average Al<sub>2</sub>O<sub>3</sub> content decreases from 12.2 wt% to 8.3 wt%.

As shown in Figures 9(b) and (e), under a constant holding time of 10 hours, the MnO content increases significantly with rising temperature, with the average content increasing from 1.6 wt% to 4.9 wt%, 9.7 wt%, and 19.7 wt%, respectively. In contrast, the Al<sub>2</sub>O<sub>3</sub> content decreases continuously, with the average content decreasing from 12.8 wt% to 11.2 wt%, 10.3 wt%, and 8.0 wt%, respectively. The variation in CaO and MgO contents is similar: after isothermal heat treatment of the control sample at 1000°C for 10 hours, both CaO and MgO contents decrease, with the average CaO content decreasing from 13.3 wt% to 7.8 wt%, and the average MgO content decreasing from 5.9 wt% to 3.3 wt%. However, when the heat treatment temperature is further increased

to 1100°C and 1200°C, no significant change is observed in the contents of CaO and MgO. After subjecting the control sample to heat treatment at 1000°C for 10 hours, the SiO<sub>2</sub> content initially increases, with the average content rising from 66.4 wt% to 72.7 wt%. However, as the temperature is further increased to 1100°C and 1200°C, the SiO<sub>2</sub> content decreases, with the average content decreasing to 70.1 wt% and 60.5 wt%, respectively.

When the holding time is fixed at 12 hours, the MnO content increases with increasing heat treatment temperature, with the average content rising from 1.6 wt% to 5.3 wt%, 8.3 wt%, and 19.3 wt%, respectively. The changes in CaO and MgO contents follow a similar trend: after heat treatment at 1000°C for 12 hours, both CaO and MgO contents decrease, with the average CaO content decreasing from 13.2 wt% to 9.8 wt%, and the average MgO content decreasing from 5.9 wt% to 3.3 wt%. However, when the heat treatment temperature is adjusted to 1100°C and 1200°C, with the holding time fixed at 12 hours, both CaO and MgO contents initially increase and then decrease. The average CaO content first increases to 12.2 wt% before decreasing to 7.9 wt%, while the average MgO content first increases to 5.7 wt% and then decreases to 3.8 wt%. The Al<sub>2</sub>O<sub>3</sub> content in the steel sample remains nearly constant after heat treatment at 1000°C and 1100°C for 12 hours, while at 1200°C, the Al<sub>2</sub>O<sub>3</sub> content decreases, with the average content dropping from 12.2 wt% to 7.9 wt%. After heat treatment at 1000°C for 12 hours, the SiO<sub>2</sub> content initially increases from 66.4 wt% to 68.6 wt%. However, as the temperature is raised to 1100°C and 1200°C, the average SiO<sub>2</sub> content first decreases to 61.5 wt% and then remains relatively stable.

During the heat treatment process, the composition of the multiphase composite oxide inclusions undergoes changes, indicating that optimal heat treatment conditions can be used to adjust the inclusion composition in Si-Mn deoxidized steel. Previous studies have shown that the changes in the composition of oxide inclusions in Si-Mn deoxidized steel are primarily attributed to the high-temperature solid-state reactions and mutual diffusion between the steel matrix and the oxides during heat treatment<sup>[24, 25]</sup>. Under scanning electron microscopy (SEM), the non-metallic inclusions in Si-Mn deoxidized steel are primarily five-phase composite oxide inclusions consisting of CaO-SiO<sub>2</sub>-Al<sub>2</sub>O<sub>3</sub>-MgO-MnO. However, FeO is also present in the actual silicon-manganese deoxidation products<sup>[13]</sup>. According to experimental results, the MnO content in the inclusions of the LX82A cast billet increases after heat treatment. This observation is consistent with previous studies, which suggest that when FeO is present in the inclusions, reactions between the inclusions and the steel matrix lead to an increase in MnO content<sup>[25]</sup>. This, in turn, widens the Mn-depleted zone at the inclusion-matrix interface, reduces austenite stability, and increases the driving force for ferrite nucleation, ultimately achieving grain refinement and improving the steel quality. Under the heat treatment conditions set in this study, with the holding time constant, the MnO content reaches its highest level at a heating temperature of 1200°C. Therefore, the heat treatment temperature should be controlled around 1200°C.

Based on relevant thermodynamic data, the oxide composition prior to heat treatment was selected, with the FeO content chosen as 3% by mass at the high-temperature equilibrium state of the alloy and oxide at 1600°C<sup>[13]</sup>. Using FactSage 8.0 software and the FToxide and FTmisc databases, the oxygen activity ( $a_{\text{O}}$ ) and FeO activity ( $a_{\text{FeO}}$ ) in the equilibrium system of silicomanganese deoxidized steel and oxide inclusions were calculated at a given temperature and oxygen partial pressure. The oxygen activity ( $a_{\text{O}}$ ) in the Si-Mn deoxidized steel at 1600°C was calculated to be  $1.73 \times 10^{-6}$ , and the FeO activity ( $a_{\text{FeO}}$ ) in the oxide was  $2.15 \times 10^{-2}$ . Due to the lack of thermodynamic data at lower temperatures in the system, the thermodynamic data at

1600°C were applied to calculate the oxygen and FeO activities at lower temperatures. The variation of  $a_O$  and  $a_{FeO}$  with temperature was thus determined for this system. As shown in Figure 10, with decreasing temperature, the oxygen activity in the steel matrix decreases sharply. When the temperature drops from 1600°C to 1200°C, 1100°C, and 1000°C, the oxygen activity ( $a_O$ ) decreases from  $1.73 \times 10^{-6}$  to  $1.14 \times 10^{-8}$ ,  $8.93 \times 10^{-9}$ , and  $1.65 \times 10^{-9}$ , respectively. When the temperature decreases from 1600°C to 1200°C, the FeO activity ( $a_{FeO}$ ) decreases from  $2.15 \times 10^{-2}$  to  $8.49 \times 10^{-3}$ . Notably, among the heat treatment temperatures set in this study, the FeO activity reaches its lowest value at 1200°C.

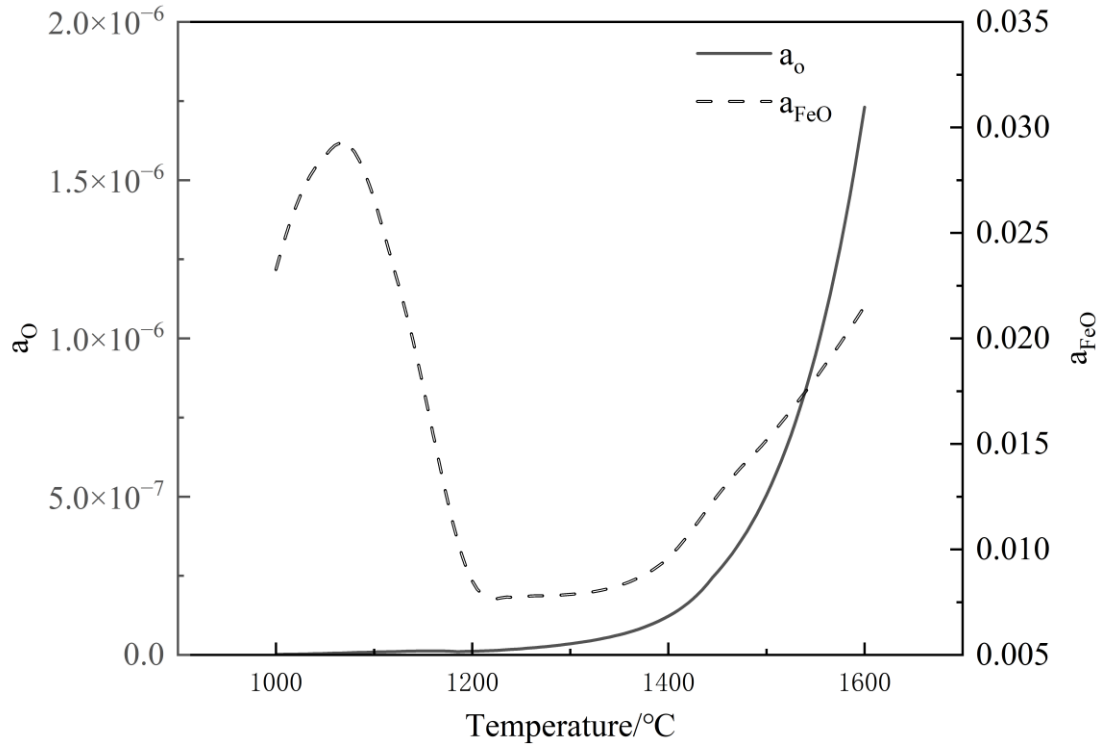


Fig. 10 The variation of oxygen activity in steel and FeO activity in inclusions with temperature during equilibrium

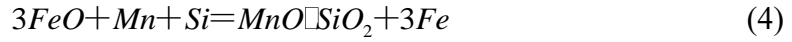
Based on the relevant literature<sup>[24, 25]</sup> and the thermodynamic calculations described above, the variation in  $SiO_2$  and  $MnO$  content in this experiment can be attributed to the following factors: When the heat treatment temperature is below 1600 °C, the equilibrium at the interface between the steel matrix and the oxide is disrupted, leading to a decrease in the oxygen activity in the steel matrix and a reduction in the FeO activity in the oxide. When the oxygen activity decreases, the excess oxygen within the Si-Mn deoxidized steel matrix reacts with the manganese and silicon elements to form  $MnO$  and  $SiO_2$  oxides, leading to an increase in the content of  $SiO_2$  and  $MnO$  at the interface. As the activity of FeO in the oxide decreases, FeO decomposes into Fe and  $[O]$ , as illustrated by the reaction in Equation (1).



The generated oxygen diffuses to the steel matrix interface, where it reacts with silicon and manganese to form silicon-manganese oxide particles. In this process, part of the  $SiO_2$  participates in the formation of new oxides, leading to the consumption of  $SiO_2$  and a subsequent decrease in its content. The reduction in  $SiO_2$  content is most pronounced at a heat treatment temperature of 1200 °C, which coincides with the lowest FeO activity observed at this temperature. The reaction is shown in Equation (2)(3).



The entire reaction can be expressed as:



Based on the analysis of the solid-phase reaction mechanisms between the silicon-manganese deoxidized steel and oxide inclusions during the heat treatment process, a schematic of the solid-phase reaction mechanism at the steel matrix–inclusion interface is shown in Figure 11.

Previous studies<sup>[26]</sup> have confirmed that during the secondary refining process in steelmaking, the high content of CaO in the molten slag decomposes into elemental Ca and O at the steel/slag interface. Excess Ca and O diffuse from the slag into the molten steel and react with inclusions, which is considered another pathway for calcium treatment. A similar decomposition reaction of CaO may occur during heat treatment, where the diffused Ca reacts with Al<sub>2</sub>O<sub>3</sub> in the inclusions. In this experiment, the variation in CaO content is primarily observed as a decrease in concentration with increasing heat treatment temperature, reaching its lowest point at 1200°C. The variation in Al<sub>2</sub>O<sub>3</sub> content is characterized by a reduction when the heat treatment temperature reaches 1200°C. This decrease in Al<sub>2</sub>O<sub>3</sub> content may be attributed to a displacement reaction between Ca and Al<sub>2</sub>O<sub>3</sub> in the inclusions during the heat treatment at 1200°C. The MgO content remains largely unchanged and does not exhibit significant variation with respect to holding time and heating temperature. This suggests that the MgO component in the oxide inclusions within the steel remains relatively stable during the heat treatment process in this experiment.

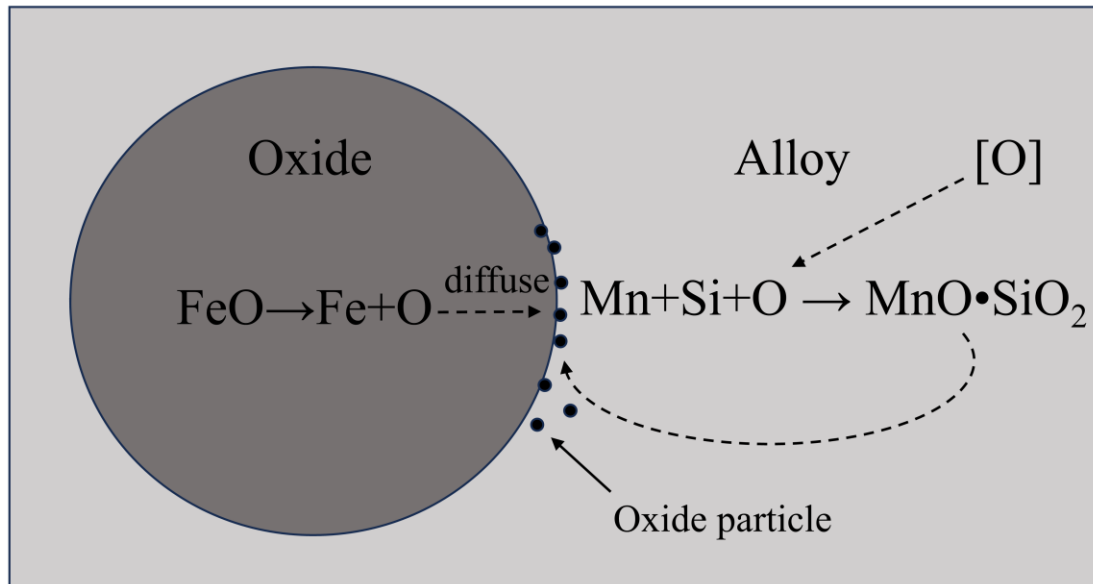


Fig.11 Interfacial reaction mechanism between steel matrix and oxide

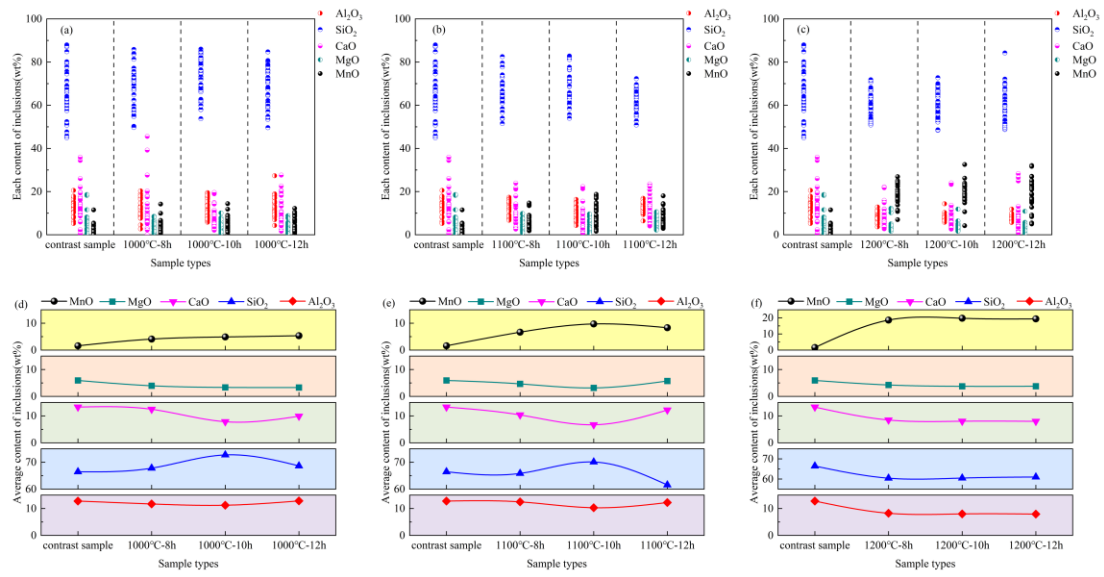


Fig. 12 Variation in the five components and the average composition of oxide inclusions in LX82A steel with holding time at the same heating temperatures: (a, d) 1000°C; (b, e) 1100°C; (c, f) 1200°C.

As shown in Figures 12(a) and (d), under a constant heating temperature of 1000°C, the contents of MgO, Al<sub>2</sub>O<sub>3</sub>, and MnO exhibit little variation as the holding time increases from 8 h to 10 h, and then to 12 h. However, when the holding time is extended from 8 h to 10 h, the average SiO<sub>2</sub> content increases from 67.8 wt% to 72.7 wt%, while the average CaO content decreases from 12.4 wt% to 7.8 wt%. When the holding time is further extended from 10 h to 12 h, the average SiO<sub>2</sub> content decreases to 68.6 wt%, and the average CaO content increases to 9.8 wt%. However, the contents of SiO<sub>2</sub> and CaO did not show significant changes when the holding time was extended from 8 h to 12 h. This indicates that under the heat treatment conditions of 1000°C and a holding time of 10 h, the extent of compositional changes in the oxide inclusions of the Si-Mn deoxidized steel is maximal.

When the heating temperature reaches 1100°C, as shown in Figures 12(b) and (e), the trends in the variations of MgO, Al<sub>2</sub>O<sub>3</sub>, and CaO contents are similar across different holding times at this temperature. As the holding time increases from 8 h to 10 h, the contents of MgO, Al<sub>2</sub>O<sub>3</sub>, and CaO slightly decrease. Specifically, the average MgO content decreases from 4.6 wt% to 3.1 wt%, the average Al<sub>2</sub>O<sub>3</sub> content decreases from 12.5 wt% to 10.3 wt%, and the average CaO content decreases from 10.3 wt% to 6.7 wt%. When the holding time is extended from 10 h to 12 h, the average contents of MgO, Al<sub>2</sub>O<sub>3</sub>, and CaO increase again, rising to 5.7 wt%, 12.2 wt%, and 12.1 wt%, respectively. The variation trends of MnO and SiO<sub>2</sub> contents are similar. As the holding time increases from 8 h to 10 h and then to 12 h, the contents first increase and then decrease. The average MnO content increases from 6.6 wt% to 9.7 wt%, before decreasing to 8.3 wt%, while the average SiO<sub>2</sub> content increases from 65.8 wt% to 70.1 wt%, and then decreases to 61.5 wt%. In summary, under the 1100°C heat treatment conditions, the contents of Al<sub>2</sub>O<sub>3</sub> and CaO reach their minimum at a holding time of 10 h, while the MnO content increases to its highest level. Therefore, among the holding times tested in this study, a holding time of 10 h is optimal for heat treatment at 1100°C.

Under the heat treatment condition of 1200°C, the composition of the inclusions shows negligible change with increasing holding time, as shown in Figures 12(c) and (f).



In summary, the composition of CaO-SiO<sub>2</sub>-Al<sub>2</sub>O<sub>3</sub>-MgO-MnO oxide inclusions in the Si-Mn deoxidized steel undergoes varying degrees of change after heat treatment, primarily due to the high-temperature solid-state reactions and diffusion between the steel matrix and the oxides during the heat treatment process. This study demonstrates the variation in the composition of non-metallic inclusions under different heat treatment temperatures and holding times, providing valuable guidance for future research on adjusting heat treatment conditions to control inclusion composition and improve steel properties. The variations in inclusion composition caused by different heating temperatures and holding times lead to the formation of a Mn-depleted zone, which facilitates the nucleation of intragranular ferrite (IGF). Further investigation into the interfacial interactions between Si-Mn deoxidized steel and inclusions is essential, and will be a key focus of future work.

#### 4.2 The morphological changes of CaO-SiO<sub>2</sub>-Al<sub>2</sub>O<sub>3</sub>-MgO-MnO composite oxide inclusions under different heat treatment conditions

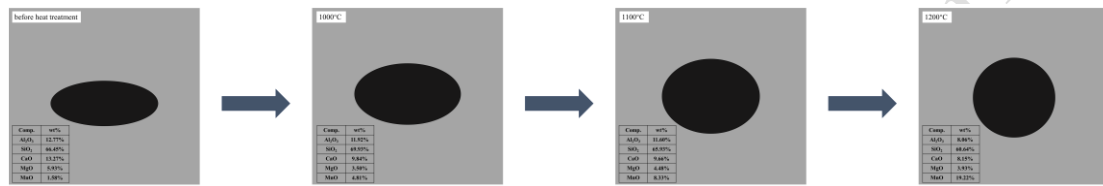


Fig. 13 Schematic diagram of oxide inclusion deformation under different heat treatment conditions

According to the experimental results in section 3.2, the shape of oxide inclusions in steel shows little change with the prolongation of holding time. However, as the heat treatment temperature increases, the inclusions gradually transition from elliptical to spherical. Therefore, the average composition of the oxide inclusions under the heat treatment temperatures set in this study is shown in Figure 13. As the heat treatment temperature increases, CaO may undergo a decomposition reaction. The diffused Ca elements can react with Al<sub>2</sub>O<sub>3</sub> in the inclusions, leading to a continuous reduction in the content of CaO and Al<sub>2</sub>O<sub>3</sub> in the oxide inclusions. This represents an alternative pathway for calcium treatment. Calcium treatment can modify oxide inclusions with a high Al<sub>2</sub>O<sub>3</sub> content by lowering their melting point, addressing nozzle clogging issues, and altering the morphology of clustered or string-like Al<sub>2</sub>O<sub>3</sub> to form spherical calcium aluminate. Using FactSage 8.0 software to calculate the melting points of oxide inclusions at different heat treatment temperatures, as shown in Table 2, it can be observed that under the set heat treatment temperature conditions, the melting point of the oxide inclusions decreases with the increase in temperature. The lowest melting point of the oxide inclusions, 1456°C, is reached at 1200°C. Previous studies<sup>[26]</sup> have indicated that the deformability of inclusions in curtain wire steel increases as the ratio of  $w(\text{Al}_2\text{O}_3 + \text{MgO}) / w(\text{SiO}_2 + \text{MnO})$  decreases. As observed from the average composition of oxide inclusions at different heat treatment temperatures in Figure 13, the ratio of  $w(\text{Al}_2\text{O}_3 + \text{MgO}) / w(\text{SiO}_2 + \text{MnO})$  is lowest at 1200°C, suggesting that oxide inclusions at this temperature exhibit improved deformability. As the heat treatment temperature increases, the oxide inclusions gradually change from an elliptical to a more circular shape, ultimately adopting a regular circular form at 1200°C. In this study, to enhance the deformability of the oxide inclusions in the steel, reduce

the occurrence of stress concentration issues in subsequent materials, and improve the mechanical properties of the material, the heat treatment temperature should be controlled near 1200°C.

Table 2 The melting points of oxide inclusions at different heat treatment temperatures

Heat treatment temperature	0°C	1000°C	1100°C	1200°C
melting point	1394°C	1508°C	1459°C	1456°C

## 5 Conclusion

In this study, the morphological and compositional changes of oxide inclusions in Si-Mn deoxidized steel were examined at three heat treatment temperatures (1000°C, 1100°C, and 1200°C) with holding times of 8, 10, and 12 hours. The results were compared with those of untreated steel samples, leading to the following conclusions.

(1) As the heat treatment temperature increases, the shape of oxide inclusions in steel shifts from elliptical to spherical. At 1200°C, the inclusions are mainly spherical, and holding time has little effect on their morphology. The oxide inclusions at 1200°C show improved deformability and a lower melting point.

(2) In untreated steel samples, the inclusions primarily belong to the CaO-SiO<sub>2</sub>-Al<sub>2</sub>O<sub>3</sub> system. After heat treatment, both the temperature and holding time induce a transformation of the oxide inclusions in Si-Mn deoxidized steel from the CaO-SiO<sub>2</sub>-Al<sub>2</sub>O<sub>3</sub> system to the MnO-SiO<sub>2</sub>-Al<sub>2</sub>O<sub>3</sub> system. As the temperature and holding time increase, the quantity of inclusions transitioning to the MnO-SiO<sub>2</sub>-Al<sub>2</sub>O<sub>3</sub> system also increases. At 1200°C, the oxide inclusions are predominantly transformed into the MnO-SiO<sub>2</sub>-Al<sub>2</sub>O<sub>3</sub> system, exhibiting a more concentrated pattern in the ternary phase diagram, which indicates a more homogeneous composition of the inclusions.

(3) When the holding time is constant, the MnO content in the inclusions increases with the heat treatment temperature. The SiO<sub>2</sub> content first increases and then decreases, with 1000°C as the inflection point. At 1200°C, the contents of CaO and Al<sub>2</sub>O<sub>3</sub> significantly decrease, while the MgO content remains stable. A heating temperature of 1200°C favors calcium treatment and the formation of a Mn-depleted zone, improving steel quality and performance. Thus, heat treatment temperature should be controlled around 1200°C.

(4) At heat treatment temperatures of 1000°C and 1100°C, with a fixed holding time of 10 hours, the oxide composition shows the greatest variation. After 10 hours, SiO<sub>2</sub> content increases, while CaO content decreases. At 1100°C, Al<sub>2</sub>O<sub>3</sub> and CaO reach their lowest levels, and MnO content peaks. Thus, a holding time of 10 hours at 1100°C is optimal. At 1200°C, the average content of the five components in Si-Mn deoxidized steel remains largely unchanged with increased holding time.

### Acknowledgments:

We would like to express our sincere gratitude to Dr. Qi Xu for his invaluable suggestions and guidance in the revision of this thesis. Special thanks to the staff at the Room 721, Steel Building, Wuhan University of Science and Technology for their technical assistance during the experimental phase.

### Funding:

This work was financially supported by the National Natural Science Foundation of China (52404350, 52274341), Research Project of Hubei Provincial Department of

Science and Technology (2024CSA083, 2024EHA001), Research Project of Hubei Provincial Department of Education (D20231101).

Conflict of Interest:

The authors declare that they have no conflict of interest.

#### **Data Availability Statement**

The data generated and analyzed during the current study are not publicly available due to proprietary information but are available from the corresponding author on reasonable request

#### **Author contribution statement**

Xinlong Nie conceived and designed the study, analyzed the data, and wrote the manuscript; Xinlong Nie collected the data and contributed to the interpretation of results; Qi Xu and Xiao Xie provided valuable suggestions and revised the manuscript for intellectual content; Jianli Li supervised the project and obtained funding.

#### **References**

- [1] Liu C, Ni H, Yang S, et al. Interfacial reaction mechanism between multi-component oxides and solid alloys deoxidised by Mn and Si during heat treatment [J]. *Ironmaking & Steelmaking*, 2017, 45(3): 195-203.  
<https://doi.org/10.1080/03019233.2016.1271968>.
- [2] Song G D, Deng Z Y, Zhu M Y. Effect of Ladle Washing Operation on Non-metallic Inclusions in Tire Cord Steel: Laboratory Simulation [J]. *Metallurgical and Materials Transactions B*, 2024, 55(4): 2805-2816.  
<https://doi.org/10.1007/s11663-024-03143-w>.
- [3] Wang K P, Jiang M, Wang X H, et al. Formation Mechanism of SiO<sub>2</sub>-Type Inclusions in Si-Mn-Killed Steel Wires Containing Limited Aluminum Content [J]. *Metallurgical and Materials Transactions B*, 2015, 46(5): 2198-2207.  
<https://doi.org/10.1007/s11663-015-0411-1>.
- [4] Liu D M, Xue Z L, Song S Q. Effect of cooling rate on non-metallic inclusion formation and precipitation and micro-segregation of Mn and Al in Fe-23Mn-10Al-0.7C steel [J]. *Journal of Materials Research and Technology*, 2023, 24: 4967-4979.  
<https://doi.org/10.1016/J.JMRT.2023.04.024>.
- [5] Kim J I, Kim S J. Numerical Evaluation for Influence of Ca Treatment and Slag Composition on Compositional Changes in Non-metallic Inclusion Using Coupled Reaction Model for Ladle Treatment [J]. *Metals and Materials International*, 2024, 30(12): 1-14.  
<https://doi.org/10.1007/s12540-024-01833-3>.
- [6] Song G D, Deng Z Y, Qin F T, et al. Effect of MgO content in refining slag on the non-metallic inclusions in tire cord steel [J]. *Journal of Materials Research and Technology*, 2024, 30: 4241-4247.  
<https://doi.org/10.1016/J.JMRT.2024.04.125>.
- [7] Park J S, Park J H. Effect of Slag Composition on the Concentration of Al<sub>2</sub>O<sub>3</sub> in the Inclusions in Si-Mn-killed Steel [J]. *Metallurgical and Materials Transactions B*, 2013, 45(3): 953-960.  
<https://doi.org/10.1007/s11663-013-9998-2>.
- [8] Zhang X W, Ye Z, Wang J J, et al. Control of non-metallic inclusions and micro-structure of an Al-killed steel through adjusting titanium content [J]. *Journal of Materials Research and Technology*, 2025, 35: 5629-5636.

- <https://doi.org/10.1016/J.JMRT.2025.02.181>.
- [9] Yang S F, Wang Q Q, Zhang L F, et al. Formation and Modification of  $\text{MgO} \cdot \text{Al}_2\text{O}_3$ -Based Inclusions in Alloy Steels [J]. *Metallurgical and Materials Transactions B*, 2012, 43(4): 731-750.  
<https://doi.org/10.1007/s11663-012-9663-1>.
- [10] Zhang J, Wang F M, Li C R. Thermodynamic analysis of the compositional control of inclusions in cutting-wire steel [J]. *International Journal of Minerals, Metallurgy, and Materials*, 2014, 21(7): 647-653.  
<https://doi.org/10.1007/s12613-014-0953-2>.
- [11] Zhou B W, Li G Q, Wan X L, et al. In-situ observation of grain refinement in the simulated heat-affected zone of high-strength low-alloy steel by Zr-Ti combined deoxidation [J]. *Metals and Materials International*, 2016, 22(2): 267-275.  
<https://doi.org/10.1007/s12540-016-5301-9>.
- [12] Ono H, Ibata T. Equilibrium Relationships between Oxide Compounds in  $\text{MgO-Ti}_2\text{O}_3\text{-Al}_2\text{O}_3$  with Iron at 1873 K and Variations in Stable Oxides with Temperature [J]. *ISIJ International*, 2011, 51(12): 2012-8.  
<https://doi.org/10.2355/isijinternational.51.2012>.
- [13] Kim K-H, Kim S-J, Shibata H, et al. Reaction between  $\text{MnO-SiO}_2\text{-FeO}$  Oxide and Fe-Mn-Si Solid Alloy during Heat Treatment [J]. *ISIJ International*, 2014, 54(10): 2144-2153.  
<https://doi.org/10.2355/isijinternational.54.2144>.
- [14] Cai S, Sun J Q, He Q K, et al. 16MnCr5 gear shaft fracture caused by inclusions and heat treatment process [J]. *Engineering Failure Analysis*, 2021, 126(11): 105458.  
<https://doi.org/10.1016/j.engfailanal.2021.105458>.
- [15] Du S, Zhang S G, Wang M T, et al. High-temperature heat treatment attenuating the influence of micron-sized inclusions on the microstructure and properties of recycled Al-Zn-Mg-Cu alloy sheet [J]. *Journal of Materials Research and Technology*, 2024, 30: 4147-4158.  
<https://doi.org/10.1016/j.jmrt.2024.04.092>.
- [16] Duan Z W, Man C, Cui H Z, et al. Formation mechanism of MnS inclusion during heat treatments and its influence on the pitting behavior of 316L stainless steel fabricated by laser powder bed fusion [J]. *Corrosion Communications*, 2022, 7: 12-22.  
<https://doi.org/10.1016/j.corcom.2022.04.002>.
- [17] Lei X B, Li J L, Zeng Q, et al. Evolution of  $\text{MnO-SiO}_2\text{-Al}_2\text{O}_3\text{-MgO}$  inclusions during heat treatment at 1100 °C [J]. *Journal of Iron and Steel Research International*, 2024, 31(5): 1221-1231.  
<https://doi.org/10.1007/s42243-023-01157-3>.
- [18] Shibata H, Kimura K, Tanaka T, et al. Mechanism of Change in Chemical Composition of Oxide Inclusions in Fe-Cr Alloys Deoxidized with Mn and Si by Heat Treatment at 1473 K [J]. *Isij International*, 2011, 51(12): 1944-1950.  
<https://doi.org/10.2355/isijinternational.51.1944>.
- [19] Choi W, Matsuura H, Tsukihashi F. Changing Behavior of Non-metallic Inclusions in Solid Iron Deoxidized by Al-Ti Addition during Heating at 1473 K [J]. *Isij International*, 2011, 51(12): 1951-1956.  
<https://doi.org/10.2355/isijinternational.51.1951>.
- [20] Meng Y Q, Li J L, Wang K P, et al. Effect of the Bloom-Heating Process on the Inclusion Size of Si-Killed Spring Steel Wire Rod [J]. *Metallurgical and Materials Transactions B*, 2022, 53(4): 2647-2656.

- <https://doi.org/10.1007/s11663-022-02557-8>.
- [21] Yang W, Guo C B, Zhang L F, et al. Evolution of Oxide Inclusions in Si-Mn Killed Steels During Hot-Rolling Process [J]. Metallurgical and Materials Transactions B, 2017, 48(5): 2717-2730.  
<https://doi.org/10.1007/s11663-017-1025-6>.
- [22] Kim K-H, Shibata H, Kitamura S-y. Influence of Sulfur on the Reaction between MnO-SiO<sub>2</sub>-FeO Oxide and Fe-Mn-Si Solid Alloy by Heat Treatment [J]. ISIJ International, 2014, 54(12): 2678-2686.  
<https://doi.org/10.2355/isijinternational.54.2678>.
- [23] Liu C S, Yang S F, Kim K H, et al. Influence of FeO and sulfur on solid state reaction between MnO-SiO<sub>2</sub>-FeO oxides and an Fe-Mn-Si solid alloy during heat treatment at 1473 K [J]. International Journal of Minerals, Metallurgy, and Materials, 2015, 22(8): 811-819.  
<https://doi.org/10.1007/s12613-015-1138-3>.
- [24] 刘成松,叶飞.热处理过程中界面固相反应控制锰硅类氧化物变性的机理研究[J].金属学报, 2017, 53(01): 10-18.  
Liu C S, Ye F. Mechanism on Modification of MnO-SiO<sub>2</sub>-Type Oxide by Interfacial Solid-State Reaction During Heat Treatment[J]. Acta Metallurgica Sinica, 2017, 53(01): 10-18. (in Chinese).  
<https://doi.org/CNKI:SUN:JSXB.0.2017-01-002>.
- [25] 叶飞,刘成松,倪红卫,等.1273 K 热处理过程中 FeO 对硅锰脱氧钢中复合氧化物的影响[J].钢铁,2018,53(05):39-44+61.  
Ye F, Liu C S, Ni H W, et al. Influence of FeO on compound oxides in Si-Mn deoxidized steel during heat treatment at 1273 K[J]. Iron and Steel, 2018, 53(05): 39-44+61. (in Chinese).  
<https://doi.org/10.13228/j.boyuan.issn0449-749x.20170457>.
- [26] 张立峰.钢中非金属夹杂物几个需要深入研究的课题[J].炼钢,2016,32(04):1-16.  
Zhang L F. Several important scientific research points of non-metallic inclusions in steel[J]. Steelmaking, 2016, 32(04): 1-16. (in Chinese).  
<https://doi.org/CNKI:SUN:LGZZ.0.2016-04-002>.

### Table captions in this article:

Table 1. The chemical composition of the tested steel(wt%).

Table 2. The melting points of oxide inclusions at different heat treatment temperatures.

### Figure captions in this article:

Figure 1. Morphology characteristics of 2-3 $\mu$ m oxide inclusions in LX82A Si-Mn deoxidized steel before heat treatment.

Figure 2. Morphology and composition surface scanning characteristics of oxide inclusions about 10  $\mu$ m in LX82A Si-Mn deoxidized steel before heat treatment.

Figure 3. Composition distribution of oxide inclusions in (a) CaO-SiO<sub>2</sub>-Al<sub>2</sub>O<sub>3</sub> and (b) MnO-SiO<sub>2</sub>-Al<sub>2</sub>O<sub>3</sub> ternary phase diagrams before heat treatment.

Figure 4. Morphology of oxide inclusions in LX82A steel under different heat treatment conditions; (1-3) 1000 °C; (4-6) 1100 °C; (7-9) 1200 °C; (1,4,7) heat preservation 8h; (2,5,8) heat preservation 10h; (3,6,9) heat preservation 12h.

Figure 5. The morphology of about 10 μm oxide inclusions in LX82A Si-Mn deoxidized steel after heat treatment at 1200 °C.

Figure 6. The composition distribution of oxide inclusions in CaO-SiO<sub>2</sub>-Al<sub>2</sub>O<sub>3</sub> and MnO-SiO<sub>2</sub>-Al<sub>2</sub>O<sub>3</sub> ternary phase diagrams after heat treatment at 1000 °C(a,d)holding for 8 h;(b,e)holding for 10 h;(c,f)holding for 12 h.

Figure 7. The composition distribution of oxide inclusions in CaO-SiO<sub>2</sub>-Al<sub>2</sub>O<sub>3</sub> and MnO-SiO<sub>2</sub>-Al<sub>2</sub>O<sub>3</sub> ternary phase diagrams after heat treatment at 1100 °C(a,d)holding for 8 h; (b,e)holding for 10 h; (c,f)holding for 12 h.

Figure 8. The composition distribution of oxide inclusions in CaO-SiO<sub>2</sub>-Al<sub>2</sub>O<sub>3</sub> and MnO-SiO<sub>2</sub>-Al<sub>2</sub>O<sub>3</sub> ternary phase diagrams after heat treatment at 1200 °C(a,d)holding for 8 h; (b,e)holding for 10 h; (c,f)holding for 12 h.

Figure 9. Variation of the five components and their average compositions of oxide inclusions in LX82A steel with heating temperature, at holding times of (a, d) 8 hours, (b, e) 10 hours, and (c, f) 12 hours.

Figure 10. The variation of oxygen activity in steel and FeO activity in inclusions with temperature during equilibrium.

Figure 11. Interfacial reaction mechanism between steel matrix and oxide.

Figure 12. Variation in the five components and the average composition of oxide inclusions in LX82A steel with holding time at the same heating temperatures: (a, d) 1000°C; (b, e) 1100°C;(c, f) 1200°C.

Figure 13. Schematic diagram of oxide inclusion deformation under different heat treatment conditions.